PCCP

Enhancement of Tetrel Bond Involving Tetrazole-TtR3 (Tt = C, Si; R = H, F). Promotion of SiR3 Transfer by a Triel Bond

Journal:	*Physical Chemistry Chemical Physics*
Manuscript ID	CP-ART-09-2022-004194.R1
Article Type:	Paper
Date Submitted by the Author:	13-Oct-2022
Complete List of Authors:	Wu, Qiaozhuo; Yantai University Xie, Xiao-Ying; Yantai University Li, Qingzhong; Yantai University Scheiner, Steve; Utah State University, Department of Chemistry and Biochemistry

Enhancement of Tetrel Bond Involving Tetrazole-TtR_3 (Tt = C, Si; R = H, F). Promotion of SiR_3 Transfer by a Triel Bond

Qiaozhuo Wu,[a] Xiaoying Xie,[a] Qingzhong Li,*[,a] Steve Scheiner*[,b]

[a] The Laboratory of Theoretical and Computational Chemistry, School of Chemistry and Chemical Engineering, Yantai University, Yantai 264005, P. R. China.

[b] Department of Chemistry and Biochemistry, Utah State University, Logan, UT 84322-0300, USA

The corresponding authors: Qingzhong Li and Steve Scheiner

E-mails: liqingzhong1990@sina.com; steve.scheiner@usu.edu

Abstract:

When attached to a tetrazole, a TtR_3 group (Tt=C, Si; R=H, F) engages in a Tt···N tetrel bond (TtB) with the Lewis base NCM (M=Li, Na). MP2/aug-cc-pVTZ calculations find that the Si···N TtB is rather strong, more than 20 kcal/mol for SiH_3, and between 46 and 53 kcal/mol for SiF_3. The C···N TtBs are relatively weaker, less than 8 kcal/mol. All of these bonds are intensified when a BH_3 or BF_3 molecule forms a triel bond to a N atom of the tetrazole ring, particularly for the C···N TtB, up to 11 kcal/mol. In these triads, the SiR_3 group displaces far enough along the line toward the base that it may be thought of as half transferred.

Keywords: Cooperativity; AIM; NBO; Hypervalent

1. Introduction

The tetrel bond (TtB) has attracted a great deal of recent attention in different fields of chemistry, materials, and biology.[1-5] This bond encompasses an attractive interaction between a group 14 atom (tetrel, Tt) as a Lewis acid and an electron donor.[6] The TtB has been applied to construct new kinds of functional materials.[7] Owing to the universality of both CH_3 and C=O groups in biomolecules, which leads to a C···O=C TtB, the TtB also modulates the structures and functions of various biomolecules,[8,9] like hydrogen bonds[10]. Other intermolecular interactions such as hydrogen and halogen bonds help catalyze organic reactions,[11,12] which thus inspires an interest in investigating the role of TtB in chemical reactions.

In most cases, heavier tetrel atoms such as Pb and Ge engage in stronger TtBs due to their lesser electronegativity and higher polarizability.[13] When adjacent to an electron-withdrawing group, its σ-hole or π-hole deepens, resulting in a stronger TtB. For this reason, electrostatic forces are thought by some to be dominant.[13] However, in some cases, a deeper σ-hole may not

necessarily give rise to a stronger TtB. For example, when a N-heterocyclic carbene (NHC) is used as a Lewis base, the carbene-tetrel bond with Si is stronger than that of the Ge analogue, despite the latter having a more prominent σ-hole.[14] It has been shown that the TtB strength depends not only on the electrostatic interaction but also on other factors such as polarization and dispersion.[13,14]

The TtB plays a role in a number of chemically important processes. The CH_3-rotation mechanism in the S_N2 reaction of $Cl^- + CH_3I$ has been analyzed in detail by using crossed molecular beam imaging and chemical dynamics calculations.[15] In this process, a structure similar to the TtB complex is found in the reactants and products. The preliminary stage of the S_N2 reaction has been likened to a TtB by Grabowski.[16] In the reaction of $N_3^- + CH_3Br \rightarrow Br^- + CH_3N_3$, a posterior stage also involves a TtB.[17] A carbon-centered, three-center, four-electron tetrel bond, $[N{-}C{-}N]^+$, formed by capturing a carbenium ion with a bidentate Lewis base, is obtained with a similar structure to the transition state geometry in the S_N2 reaction.[18] A TtB is also utilized to form a frustrated Lewis pair for H_2 activation.[19] On the other hand, H_2 molecule is also taken as an electron donor to form a TtB with SiH_3^+ and GeH_3^+.[20]

Proton transfer is an important phenomenon in biological and chemical reactions.[21] This transfer can be promoted by introducing an intermolecular interaction to a molecule containing an intramolecular hydrogen bond.[22-24] As an example, a TtB has the ability to convert a neutral amino acid into a zwitterion.[24] This promotion was realized through a beryllium bond[22] or a TtB[23] which enhances the strength of the intramolecular hydrogen bond. A TtR_3 group which participates in a TtB can likewise transfer under certain conditions. The TtB interaction in $CH_3OH\cdots NCH$ is very weak with an interaction energy of 1.3 kcal/mol.[25] This quantity is magnified to 35.5 kcal/mol if C of CH_3, H of CH_3, and H of NCH are replaced by Ge, F, and Na, respectively.[25] Adding a $BeCl_2$ molecule to the binary complex through a beryllium bond enhances the interaction energy, and a half transfer is observed for the GeF_3 group.[25] As another example, the interaction energy of the TtB interaction between $PhTtH_3$ (Tt = Si and Ge) and N-heterocyclic carbene (NHC) is less than 4 kcal/mol.[26] When the benzene ring of $PhTtH_3$ participates in a cation-π interaction with Be^{2+}, this quantity rises dramatically to 100 kcal/mol, and a complete transfer occurs.[26]

Along similar lines of repercussions of Be-bonding, it has been demonstrated that the N-H acidity of azoles is greatly enhanced through adding a $BeCl_2$ molecule to the other nitrogen atoms.[27] Strong beryllium bonds can modulate the strength of other weak interactions and can even change their properties. For example, weak halogen bonds in pyridine$\cdots$ClF complexes are significantly enhanced in the presence of beryllium bonds.[28] When beryllium bonds coexist in the same system with hydrogen or halogen bonds, the hydrogen or halogen bonds may become

ion-pair bonds and may even undergo proton transfer or halogen transfer.[29] As a result, beryllium bonds exhibit notable positive synergistic effects with other weak interactions, characterized by high cooperative energies and shorter binding distances.

While decades of study of the proton transfer process have led to a well understood set of circumstances that will lead to such a transfer, [30-38] examination of tetrel transfer remains in its infancy. A central question concerns the conditions under which a TtR_3 group can be promoted to transfer from one molecule to another. In the work mentioned above, a TtR_3 group transfers between two carbon atoms in $PhTtH_3$···carbene[26] or from O to N in TtX_3OH···NCH.[25] The N-Tt bond energy is somewhat smaller than its C-Tt counterpart, in this work, thus we place a TtR_3 group on a N atom of tetrazole to enable its subsequent transfer. The latter five-membered ring also presents the possibility of bonding to an electron acceptor at a different N-site which might cooperatively promote this transfer. Four different TtR_3 groups were considered, with Tt= C and Se, and R=H and F. In order to strengthen the ability of the partner to attract the TtR_3, a strongly electron-releasing metal atom was added to the cyano group, so that the N atom on the ensuing NCM molecule might make for a strong nucleophile, with M=Li and Na. As prior work has suggested that the T transfer can be promoted if a Lewis acid is added to the T-containing unit, the tetrazole is allowed to form a triel bond with BR_3 (R = H and F).

2. Theoretical Methods

The geometries of all complexes and their monomers were optimized at the MP2/aug-cc-pVTZ level.[39] To ensure that all structures represent true minima on the potential energy surface, harmonic frequency calculations were performed at the same level and revealed no imaginary frequencies. The interaction energies were calculated as the difference between the energy of the complex and the sum of the monomers with their geometries frozen as in the complex. The interaction energy of tetrel bond in the ternary complex was obtained with the similar method, but the energies of triel-bonded dimer and MCN monomer were subtracted. The binding energy is similar except that the monomers were taken in their fully optimized geometries. Both terms were corrected for basis set superposition error (BSSE) using the counterpoise method proposed by Boys and Bernardi.[40] All calculations were performed with the Gaussian 09 program.[41]

The molecular electrostatic potential (MEP) of each monomer and complex was calculated using wave function analysis surface analysis software (WFA-SAS)[42] on the 0.001 a.u. isodensity surface at the MP2/aug-cc-pVTZ level. Electron density, Laplacian, and total energy density at bond critical points (BCP) were obtained by the multiwfn program[43] using the Bader theory of atoms in molecules (AIM).[44] Analysis of orbital interactions and charge transfer between orbitals was performed using the natural bond orbital (NBO) method [45] The energy

decomposition of each complex was accomplished via the GAMESS program[46] using a fixed-domain molecular orbital energy decomposition analysis [47] at the MP2/aug-cc-pVTZ level.

3. Results

MEPs of Monomers

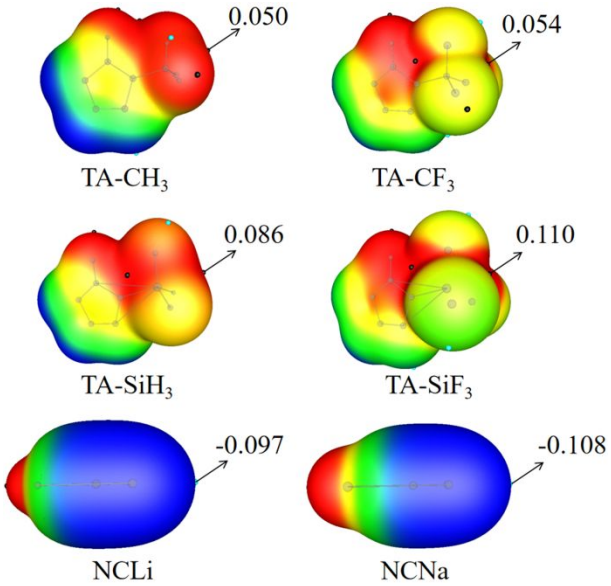

Fig.1 MEP maps of monomers. Color ranges are: red, greater than 0.02; yellow, between 0.02 and 0; green, between -0.02 and 0; blue, less than -0.02. All are in a.u.

The MEP diagrams for the Lewis acids TA-CH_3 and TA-CF_3 are represented in the top row of Fig. 1 (where TA stands for tetrazole), while their Si counterparts are contained in the second row. Each unit displays a σ-hole on the extension of its N-Tt bond, as shown by the red region on the right. The magnitude and location of the maximum value of MEP on the 0.001 a.u. isodensity surface, $V_{s,max}$, is indicated on each graph. This hole is considerably deeper for Si than for C. F substitution deepens the σ-hole; very little for Tt=C but by much more for Si. As is visible in the third row of Fig. 1, the N atom of NCLi and NCNa is surrounded by a blue negative area. The minimum on this surface is roughly 0.1 a.u., somewhat larger in magnitude for Na as compared to Li.

For purposes of completeness, in addition to these primary sites, there are a number of secondary extrema on these surfaces. The Tt atom has three other σ-holes that are directed along the antipodes of each Tt-H/F bond. As indicated in Fig. S1, these σ-holes are shallower than the primary N-Tt site. The three N atoms in each TA-TtR_3 are surrounded by a negative blue region, also visible in Fig. S1.

Binary Complexes

Contact between the deepest σ-hole on the Tt atom and the negative N atom of NCM leads to formation of a tetrel bond (TtB) between them in the complexes displayed in Fig. 2. The intermolecular R(Tt···N) distance is contained in these diagrams. This distance is roughly 3.0 Å for the CH_3 systems, and is a bit longer at 3.2 Å for CF_3. There is a very substantial contraction in this distance down to 2.0 – 2.2 Å when C is mutated to Si. This shortening is particularly striking in view of the larger size of the Si atomic radius. This can be attributed to the large interaction energy in the SiR_3 complex and the property of partially covalent interaction for the Si···N TtB in the following sections.

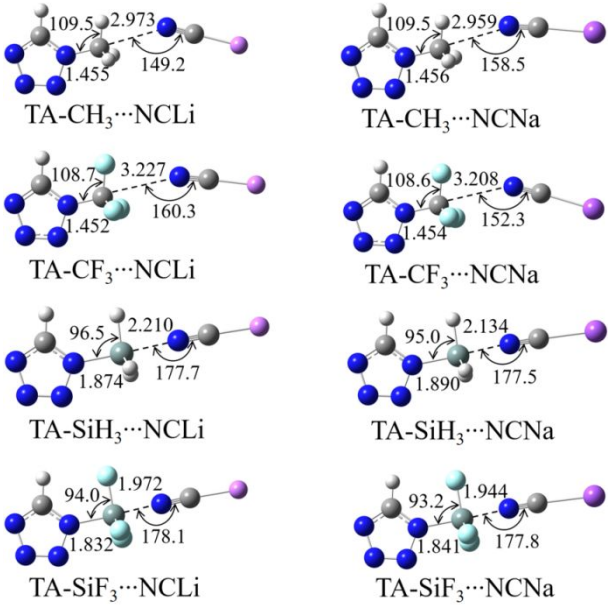

Fig.2 Optimized structures of binary complexes, marked with the mean of the three angles N-Tt-R (α, deg), Tt···N-C angle (β, deg), N-Tt bond length (R_1, Å), and Tt···N distance (R_2, Å).

Table 1 Change of N-Tt bond length (ΔR_1) relative to the isolated monomer, difference between Tt···NCM distance and N-Tt bond length ($R_2 - R_1$), interaction energy (E_{int}), binding energy (E_b), and deformation energy (DE) in the binary complexes. Energies in kcal/mol and distances in Å

	ΔR_1	$R_2 - R_1$	E_{int}	E_b	DE
TA-CH_3···NCLi	0.005	1.518	-6.72	-6.66	0.06
TA-CH_3···NCNa	0.006	1.503	-7.63	-7.54	0.09
TA-CF_3···NCLi	0.014	1.775	-3.79	-3.55	0.24
TA-CF_3···NCNa	0.015	1.754	-4.33	-4.02	0.31
TA-SiH_3···NCLi	0.079	0.336	-21.21	-13.86	7.35
TA-SiH_3···NCNa	0.095	0.244	-26.69	-16.88	9.81
TA-SiF_3···NCLi	0.084	0.140	-45.85	-18.10	27.75
TA-SiF_3···NCNa	0.093	0.103	-53.36	-22.48	30.88

TA-GeF_3···NCNa	0.076	0.098	-52.82	-27.30	25.52

The formation of each dyad leads to a certain amount of distortion of the internal geometry of the Lewis acid. The internal R(Tt-N) bond length R_1 undergoes a stretch, displayed as ΔR_1 in Table 1. This stretch is only 0.005 Å for CH_3, triples to 0.015 Å for CF_3, and rises to 0.08 to 0.09 Å for the SiR_3 units. Despite its elongation, R_1 remains comfortably smaller than the intermolecular R_2 for Tt=C, as is obvious from the (R_2–R_1) measures of 1.5-1.7 Å in Table 1. However, this difference is reduced to less than 0.4 Å for Si, and as small as 0.10 Å for TA-SiF_3···NCNa. Along with this internal bond elongation there is an opening of the umbrella angle α(NTtR) from a tetrahedral configuration for the C systems to a more nearly perpendicular 95° for Tt=Si. That is, the SiR_3 unit takes on a quasiplanar structure.

The succeeding columns of Table 1 denote the energetics of the complexation. The smallest interaction energies of 4 kcal/mol are associated with the CF_3 substituents, and are roughly doubled for CH_3. Note that this trend is opposite to an expectation based on the deeper σ-hole for the latter substituent. But there is a much larger enhancement when C is replaced by Si, with interaction energies varying from 21 to 53 kcal/mol, reaching its upper limit for SiF_3. It is intriguing to note that the conversion from CH_3 to CF_3 reduces this interaction energy, but the fluorosubstitution has the opposite effect of raising this quantity for the Si analogues, and by quite a bit. One trend all systems share in common is that the mutation from NCLi to NCNa enhances the interaction. The energetics correlates quite well with the geometric parameters. The strongest binding results in the shortest intermolecular contacts, the largest internal bond stretch and the greatest opening of the umbrella angle. The quite different interaction energies between TA-SiR_3 and TA-CR_3 complexes are also confirmed at the CCSD(T)/aug-cc-pVTZ level. For instance, the difference of the corresponding interaction energy is 13.48 kcal/mol for TA-SiH_3···NCLi and TA-CH_3···NCLi. This shows that the effect of triples does not affect this relative trend, consistent with data in Refs. 14 and 16.

These internal perturbations caused by the complexation raise the energy of the Lewis acid by an amount known as the deformation energy, listed as DE in the penultimate column of Table 1. These deformation energies are rather small for the weakly bound CR_3 dyads, but much larger for Si, where the N-Si bond stretches by nearly 0.1 Å and the SiR_3 unit becomes nearly planar. These deformation energies reduce the magnitude of the binding energy so that the full energy change E_b for the complexation from optimized monomers to dimer in the last column of Table 1 are not quite as negative as E_{int}. The largest binding energy of 22.5 kcal/mol arises in connection with the combination of NCNa with TA-SiF_3.

Table 2. Electron density (ρ), Laplacian ($\nabla^2\rho$), and energy density (H) at the Tt···N and N-Tt BCPs in the binary complexes, all in a.u.

	Tt···N			N-Tt		
	ρ	$\nabla^2\rho$	H	ρ	$\nabla^2\rho$	H
TA-CH_3···NCLi	0.0084	0.0413	0.0023	0.2533	-0.3595	-0.3738
TA-CH_3···NCNa	0.0090	0.0429	0.0023	0.2500	-0.3448	-0.3719
TA-CF_3···NCLi	0.0049	0.0268	0.0015	0.2983	-1.1982	-0.4145
TA-CF_3···NCNa	0.0051	0.0279	0.0015	0.2969	-1.1900	-0.4126
TA-SiH_3···NCLi	0.0375	0.1341	-0.0071	0.0930	0.4461	-0.0346
TA-SiH_3···NCNa	0.0441	0.1823	-0.0083	0.0893	0.4253	-0.0322
TA-SiF_3···NCLi	0.0660	0.3299	-0.0166	0.1083	0.4903	-0.0498
TA-SiF_3···NCNa	0.0714	0.3590	-0.0197	0.1061	0.4779	-0.0481
TA-GeF_3···NCNa	0.0897	0.3142	-0.0345	0.1265	0.3688	-0.0668

AIM analysis of the topology of the electron density of these complexes is consistent with the energetic trends. The first three columns of Table 2 refer to the bond critical point of the intermolecular Tt···N bond. The density at this point is fairly small for the CH_3 complexes, and even smaller for CF_3, all less than 0.01 a.u.. This quantity is ramped up for Tt=Si, especially for the SiF_3 substituents, where it exceeds 0.06 a.u.. The Laplacian of the density obeys a similar trend, as does the energy density H. The latter quantity switches sign from positive to negative upon exchanging C for Si, indicating an element of covalency enters the intermolecular bond. All of these quantities are much larger for the internal N-Tt bond, which is clearly covalent, with ρ=0.1 a.u. or larger, and negative H. However, one can note a waning of the degree of covalency in this bond for Tt=Si, with ρ dropping below 0.1 a.u., a positive $\nabla^2\rho$, and a much reduced magnitude of H. These trends are consistent with the NCI diagrams in Fig. S2. The green region in the figure is consistent with a weak C···N TtB, while the blue region enclosed by red is consistent with partially covalent N-Si and Si···N interactions.

An important feature of TtB and related noncovalent interactions is the transfer of a certain amount of charge from the electron donor unit to the acceptor. The first column of Table S1 shows that this transfer (CT) is very small in the -CR_3-containing binary complexes, all less than 0.004 e, but this quantity is greatly amplified in the SiR_3 counterparts. Again, this pattern is fully consistent with the energetics of dimerization. In addition to the total charge transfer between molecules, this phenomenon can be subdivided into transfers between individual molecular orbitals via the NBO protocol. When the -CR_3 group acts as a Lewis acid, the principal transfer

takes place from the N lone pair of NCM to the $\sigma^*_{N\text{-}C}$ antibonding orbital. The second-order perturbation energy associated with this transfer is denoted $E_1^{(2)}$ and can be seen in Table S1 to be rather small, particularly for the weakest dimers involving -CF_3, where it is less than 0.2 kcal/mol. There is a secondary transfer to the $\sigma^*_{C\text{-}H}$ orbitals of the CH_3 group, but these are essentially insignificant. Mutation to the SiH_3 group aggravates these transfers by an order of magnitude, even approaching 50 kcal/mol. Even the secondary transfers to the peripheral antibonding orbitals are expanded. For the TA-SiF_3···NCNa system, the cumulative transfer of $LP_N \rightarrow \sigma^*_{Si\text{-}H}$ orbitals can rise to 40 kcal/mol, but their average is still smaller than $E_1^{(2)}$, indicating that for the SiH_3 system the $LP_N \rightarrow \sigma^*_{Si\text{-}F}$ orbital interaction is dominant, and Fig. 3 illustrates the overlap of the orbitals involved in these important transfers.

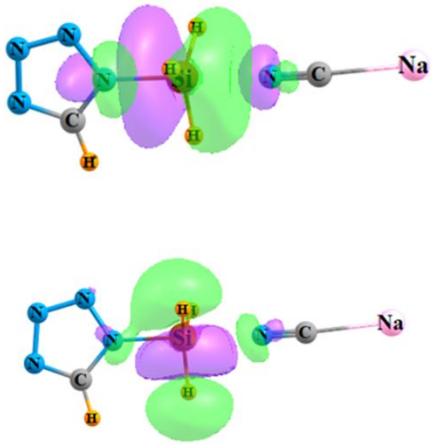

Fig. 3 Disposition of NBO orbitals involved in the $Lp_N \rightarrow \sigma^*_{N\text{-}Si}$ (top) and $Lp_N \rightarrow \sigma^*_{Si\text{-}H}$ (down) orbital interactions in TA-SiH_3···NCNa.

Another window into the forces contributing to the formation of the bonding arises by partitioning the total interaction energy into its physically meaningful components. The results of this decomposition into electrostatic (E^{ele}), exchange (E^{ex}), repulsion (E^{rep}), polarization (E^{pol}), and dispersion (E^{disp}) energies are collected in Table 3. The E^{ele} term is mainly derived from the classical Coulomb interaction of the occupied orbitals of one monomer with those of another monomer. The E^{pol} term contains all classical induction, exchange-induction, etc., from the second order up to infinity, and charge transfer is contained in the E^{pol} term. The E^{ex} and E^{disp} terms are defined using the changes in the exchange and correlation functional on going from monomers to supermolecule. E^{rep} results from the Pauli exclusion principle. It may be seen first that electrostatic and exchange effects contribute the largest amounts, comparable to one another. For the Tt=C complexes, dispersion is a larger factor than is polarization, although both are minor contributors. All components enlarge when C is changed to Si, consistent with the overall

stronger bonds and the much closer approach of the two subunits in the latter case. The electrostatic term rises by an order of magnitude and polarization is magnified by an even larger factor, reaching up near 60 kcal/mol. Dispersion, plays a much more minor role, and even smaller for SiF_3 than for CF_3. The particularly large rise in repulsion energy on adding the three F atoms to Si can be attributed to their repulsion with the N atom.

Table 3. Electrostatic (E^{ele}), exchange (E^{ex}), repulsion (E^{rep}), polarization (E^{pol}), and dispersion energies (E^{disp}) as well as the total interaction energy (E_{total}) in the binary complexes, all in kcal/mol

	E^{ele}	E^{ex}	E^{rep}	E^{pol}	E^{disp}	E_{total}
TA-CH_3···NCLi	-7.38	-5.83	9.74	-1.37	-1.89	-6.72
TA-CH_3···NCNa	-8.38	-6.43	10.74	-1.66	-1.85	-7.58
TA-CF_3···NCLi	-4.39	-4.38	7.67	-0.88	-1.82	-3.80
TA-CF_3···NCNa	-5.05	-4.93	8.66	-1.08	-1.89	-4.31
TA-SiH_3···NCLi	-44.20	-62.18	116.96	-25.92	-6.33	-21.68
TA-SiH_3···NCNa	-54.96	-75.11	142.96	-33.85	-6.09	-27.05
TA-SiF_3···NCLi	-80.66	-81.27	167.89	-51.02	-1.50	-46.55
TA-SiF_3···NCNa	-90.12	-86.96	180.43	-56.85	-0.37	-53.87
TA-GeF_3···NCNa	-94.97	-85.62	181.39	-54.49	1.07	-52.61

Ternary Complexes

It was shown earlier that placement of a cation in the vicinity of the Lewis acid draws electron density away from the latter, deepening the σ-hole on the T atom, and making it a stronger acid in its own right. One might expect a similar effect might occur if the cation is replaced by another sort of electron-withdrawing agent. The BH_3 molecule is known to engage in fairly strong interactions in which electron density is drawn into the vacant *p*-orbital of the electron-deficient B atom. Similar sorts of effects are anticipated if the H atoms are replaced by electron-withdrawing F atoms, viz. BF_3. Each of these two molecules was allowed to interact with either N atom of the tetrazole ring, exclusive of the N immediately adjacent to the TtR_3 group.

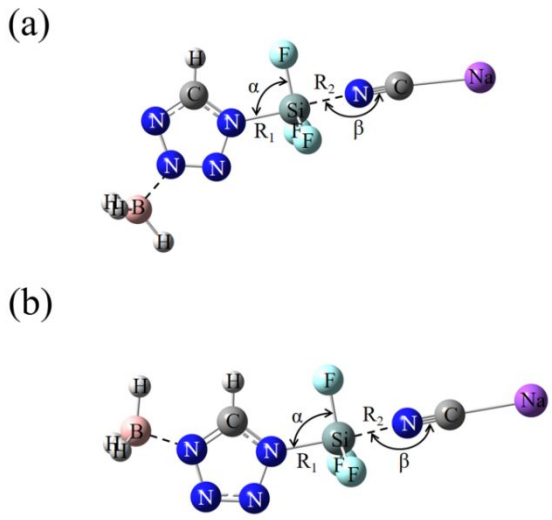

Fig. 4 Schemes of ternary complexes of (a) 3-BH_3···TA-SiF_3···NCNa and (b) 4-BH_3···TA-SiF_3···NCNa.

The geometry of the resulting triad with BH_3 is pictured in Fig. 4 with the BH_3 located near each of the two N atoms of the tetrazole. As anticipated, the addition of either BR_3 ligand deepens the Tt σ-hole. V_{max} rises by some 0.02 – 0.03 a.u., as detailed in Table S2 amounting to an increase of 17-32%, and the effect of BF_3 slightly larger than BH_3. This electron density shift intensifies the tetrel bond with NCNa. The interaction energies in Table 4 follow a similar pattern as in the dyads: SiF_3 >> SiH_3 >> CH_3 > CF_3. The increase in the tetrel bond energy arising from the presence of the BR_3 in the next column of Table 4 is quite substantial, accounting for between 12 and 43% of the total. These tetrel bond energies within the triads are all fairly strong. The interaction energies involving the CH_3 group are some 10 kcal/mol, quite strong for a methyl group. The values for SiH_3 are some 4 times higher, and those for SiF_3 climb to nearly 70 kcal/mol.

Table 4. Interaction energy of tetrel bond (E_{int}, kcal/mol) and its change (ΔE_{int}, kcal/mol) relative to the binary analogue, average of three N-Tt-X angles (α, deg), Tt···N-C angle (β, deg), N-Tt bond length (R_1, Å), Tt···NCM distance (R_2, Å) and its difference (ΔR_2) relative to the binary analogue in the ternary complexes

	E_{int}	ΔE_{int}	α	β	R_1	R_2	ΔR_2	$R_2 - R_1$
3-BH_3···TA-CH_3···NCNa	-9.67	-2.04	109.3	176.3	1.452	2.843	-0.116	1.391
4-BH_3···TA-CH_3···NCNa	-10.05	-2.42	109.2	167.9	1.460	2.902	-0.057	1.442
3-BF_3···TA-CH_3···NCNa	-10.63	-3.00	109.2	175.8	1.453	2.822	-0.137	1.369
4-BF_3···TA-CH_3···NCNa	-10.96	-3.33	109.1	173.2	1.461	2.887	-0.071	1.426

3-BH_3···TA-CF_3···NCNa	-6.73	-2.40	107.9	150.1	1.467	3.122	-0.086	1.655
4-BH_3···TA-CF_3···NCNa	-6.66	-2.33	107.9	167.3	1.467	3.125	-0.083	1.658
3-BF_3···TA-CF_3···NCNa	-7.61	-3.28	107.7	158.6	1.473	3.092	-0.116	1.619
4-BF_3···TA-CF_3···NCNa	-7.51	-3.18	107.7	173.3	1.472	3.096	-0.112	1.624
3-BH_3···TA-SiH_3···NCNa	-35.58	-8.89	92.7	176.6	1.929	2.058	-0.076	0.129
4-BH_3···TA-SiH_3···NCNa	-35.59	-8.90	92.7	178.6	1.929	2.058	-0.076	0.129
3-BF_3···TA-SiH_3···NCNa	-39.14	-12.45	91.9	176.4	1.946	2.036	-0.098	0.090
4-BF_3···TA-SiH_3···NCNa	-38.91	-12.22	92.0	179.1	1.944	2.037	-0.097	0.093
3-BH_3···TA-SiF_3···NCNa	-62.36	-9.00	91.9	177.0	1.866	1.917	-0.027	0.051
4-BH_3···TA-SiF_3···NCNa	-60.74	-7.38	91.9	178.5	1.845	1.897	-0.047	0.052
3-BF_3···TA-SiF_3···NCNa	-65.89	-12.53	91.4	176.6	1.877	1.908	-0.036	0.031
4-BF_3···TA-SiF_3···NCNa	-65.70	-12.34	91.4	178.9	1.875	1.909	-0.035	0.034
3-BF_3···TA-GeF_3···NCNa	-63.95	-11.13	91.7	176.7	1.931	1.968	-0.029	0.037

The α angle which reflects the pyramidal character of the TtR_3 group remains close to 109° for the CR_3 substituents, but comes even closer to 90° in the triads involving SiR_3 than was observed in the dyads. The presence of the BR_3 unit also pulls the NCNa base in closer to the Tt. This contraction is listed as ΔR_2 in Table 4 and is as much as 0.14 Å. The last column of Table 4 expresses the large distinction between the internal and external Tt-N bond lengths in the CR_3 complexes, as these two distances differ by roughly 1.5 Å. The situation is quite different, however, for the Si analogues. The external bond length to NCNa differs from the internal distance by only 0.03 – 0.13 Å. When coupled with the α angle that is close to 90°, these systems resemble a hypervalent Si atom. The two N atoms occupy apical positions of a trigonal bipyramid, and the equatorial sites are taken up by the three R substituents, H or F. An equivalent perspective of this situation might be described as a half transfer of the SiR_3 group from the tetrazole to the NCNa unit.

The enhancement of the TtB and the weakening of the internal N-T bond are also reflected in the AIM measures of the electron density topology. As indicated in Table S3, both ρ and $\nabla^2\rho$ of the Tt···N BCP are amplified for the ternary complex relative to the corresponding dyad, while the ρ at the internal N-Tt BCP is reduced. The presence of the BR_3 unit raises the total charge being transferred to the tetrazole from the NCNa, This CT amplification listed in Table S4 is variable, ranging up to as much as a 40% increase. Also ramped up by the presence of the extra Lewis acid are the transfers between individual molecular orbitals, which are displayed in Table S5.

4. Discussion

Some work in the literature offers a yardstick by which to compare some of the data

presented here. First with regard to the triel bond, it has been demonstrated that BF_3 contains a larger π-hole above the B than does BH_3, although the latter engages in a stronger triel bond.[48] This conclusion carries over to the triel bonds formed by these two molecules with the N atom of TA-TtR_3. For instance, the B···N distance is 1.674 Å and 1.606 Å, respectively, when the N atom of TA-SiH_3 binds with BF_3 and BH_3.

The TtB formed by -CR_3 is usually very weak and the σ-hole on the C atom is especially shallow.[49,50] However, incorporation of electron-withdrawing substituents can strengthen the TtB. For example, the C atom in 3,3-dimethyl-tetracyanocyclopropane can form a strong TtB with tetrahydrofuran (~11 kcal/mol) due to the presence of the four CN substituents.[51] Conversely, placement of electron-releasing substituents on the Lewis base can also strengthen the TtB. While the interaction energy of the complex pairing CH_3F with C_2H_2 is 1.2 kcal/mol, it is increased five-fold when the two H atoms of C_2H_2 are replaced by Na atoms.[52] With particular regard to the tetrazole subunit considered here, it appears to be a strong tetrel bond donor. For instance, the interaction energy is 2.5 kcal/mol when CH_3OH forms a TtB with NCNa,[25] but triples if CH_3OH is replaced by TA-CH_3. This rise is due in part to the deeper σ-hole in the latter molecule, 0.07 a.u., as compared to only 0.014 a.u. for CH_3OH.

The superior strength of tetrel bonds involving Si has been noted on numerous occasions in the past,[16,53-59] even in an intramolecular setting.[60] Pyridine-SiF_3 binds much more strongly to NH_3 than does its C-analogue,[61] with respective interaction energies of 26 and 1 kcal/mol. A similarly large disparity occurs if the pyridine ring is replaced by furan.[61] Protonation of the Lewis acid enhances the tetrel bond strength, and shortens the Si···N distance.[61] Placing the TtF_3 group on a trisubstituted phenyl ring [62] provided a further evidence for the much stronger tetrel bonding of Si relative to C. In general, SiR_3 forms a weaker TtB than its Ge-analogue according to the σ-hole magnitude. However, this is not true when these σ-holes meet with strong Lewis bases such as a N-heterocyclic carbene (NHC).[14] This case holds true for the strong Lewis base NCM (M=Li, Na) since the interaction energy of TA-GeF_3···NCNa is smaller than that of SiF_3 analogue. The addition of BF_3 to the N atom of tetrazole does not change this case.

This strength extends also to bonding to π-holes generated on Si [63,64] when in a trivalent situation as in F_2SiO [23] or H_2SiO [65] where the N···Si interaction with substituted pyridines exceeds 30 kcal/mol and the distance between the two atoms is essentially equal to the sum of their covalent radii. Like the σ-hole bonds discussed here, there is a large deformation energy, roughly 8 kcal/mol in these cases. Other calculations [66,67] have reinforced the idea of π-hole tetrel bonds and shown they can be stronger than their σ-hole counterparts, even though the former do not have deeper holes.

It has long been understood that cooperativity can be a powerful force in strengthening H-

bonds [68-70] as each unit serves simultaneously as both an electron donor in one bond and an acceptor in another. This same phenomenon has been shown to be operative in other noncovalent bonds such as the TtB.[25,71] The beryllium bond is an example of a strong interaction that is commonly utilized as a second interaction to add to a binary system.[25,71] The TtB in $BeH_2\cdots TtH_3X\cdots NH_3$ (X = F, Cl, and Br; Tt = C, Si, and Ge) is reinforced by the beryllium bond,[71] since the central TtH_3X acts as both donor and acceptor. The moderately strong TtB in $SiH_3F\cdots NCH$ becomes a strong TtB in $BeH_2\cdots SiH_3F\cdots NCH$. [71] A similar effect was observed in $BeCl_2\cdots TtX_3OH\cdots NCM$ (Tt= C, Si, Ge; X = H, F; M = H, Li, Na).[25] The TtB is enhanced by the addition of the electron-accepting $BeCl_2$ at the O-atom end of the Lewis acid, raising the interaction energy to nearly 60 kcal/mol.[25] If $BeCl_2$ is changed to $MgCl_2$, the ensuing magnesium bond can also modulate the TtB in $MgCl_2\cdots TtF_3OH\cdots NCH/NH_3$/imidazole (Tt = C, Si, and Ge). [72] Besides the beryllium/magnesium bond, the triel bond is also effective in enhancing a proximate interaction, and by a surprising degree.[73] Although BF_3 forms a weaker triel bond than does BH_3, it nevertheless exerts a larger enhancing effect on the tetrel bond in the TA-CR_3 complex. In above ternary systems, the B/Be/Mg draws electron density toward itself, and this results in a reduced density on the electron acceptor molecule, making it a stronger acid and leading to a stronger TtB with the N atom of N-containing molecules.

The combination of tetrazole bound to the TtR_3 group with an electron-releasing metal atom on the NCM base leads to rather strong tetrel bonds here. Even for the normally weakly bonding CH_3 group, the TtBs amount to 7 kcal/mol, stronger than the prototypical H-bond in the water dimer. The TtB is even stronger when C is replaced by Si. The TtB of TA-SiH_3 lies between 20 and 30 kcal/mol, which is roughly doubled for SiF_3. These stronger TtBs also weaken the internal N-Si bond within the Lewis acid, but the latter bond remains shorter than the external Si⋯N distance. Even so, the difference between these two distances is fairly small, between 0.1 and 0.3 Å so one can think of these complexes as containing a fair degree of SiR_3 transfer from TA to the base.

This transfer is accentuated when a BR_3 Lewis acid is allowed to interact with a N atom of the tetrazole. The interaction energy of the TtB is amplified by up to 12 kcal/mol. The energies associated with the CH_3 group rise up above 10 kcal/mol although the group remains firmly ensconced on the tetrazole. However, the cooperativity associated with the triel bond pushes the SiR_3 even further toward the base. The external Si⋯N bond is longer than the internal bond by only 0.1 Å, and as small as 0.03 Å in some cases. The bonding in these complexes can be described alternately as either half-transferred SiR_3 or as a hypervalent trigonal bipyramid.

An earlier work [26] had documented a similar sort of half transfer of a TtR_3 group. In that case, the SiH_3 or GeH_3 group attached to a phenyl ring moved halfway toward any of a series of

bases NH_3, $NHCH_2$ and $C_3N_2H_4$ carbene when spurred to do so by the presence of a dication interacting with the phenyl ring. The stronger nucleophilicity of NCM as compared to these earlier bases can be approximated by their V_{min}. This quantity is equal to -0.097 and -0.108 a.u. for NCLi and NCNa, respectively. V_{min} is less negative for the earlier bases: -0.059 a.u. for NH_3, -0.058 a.u. for $NHCH_2$, and -0.078 a.u. for the carbene. With respect to the Lewis acids, the V_{max} of TA-CH_3 of 0.050 a.u. is considerably larger than 0.004 a.u. for $PhCH_3$. The calculations described here find that the external agent need not be as strongly electron withdrawing as a single-center dication such as Be^{2+} or Mg^{2+}. The same displacement can be occasioned by a simple neutral molecule, in this case BH_3 or BF_3 which can engage in a triel bond with the Lewis acid in question. This half-transferred structure is reminiscent of the transition state for a S_N2 reaction. However, in contrast to the latter which lies at an energy maximum, the half-transferred geometries described her represent the minimum energy conformation. At this point, the C atom is resistant to the half transfers that are characteristic of Si and Ge. Future work will attempt to identify conditions necessary for C to also participate in such a process.

When the Tt···N distance is hold at 3 Å for all binary complexes, the corresponding energy decomposition terms are listed in Table S6. Each term has a small change for the C···N interaction but varies greatly for the Si···N and Ge···N interactions. For the latter two interactions, both electrostatic and polarization terms are decreased greatly and electrostatic is still larger than polarization although the ratio of polarization to electrostatic is decreased. To have a further analysis for the effect of binding distance on the each term, TA-SiF_3···NCNa is selected as an example, where the Si···N distance varies from 2 Å to 3 Å with 0.2 Å separation, to consider the effect of the Tt···N distance on each energy contribution (Table S7). With the increase of Si···N distance, each term excluding dispersion is decreased and the ratio of polarization to electrostatic is also decreased.

The TA-TtR_3 molecule suffers a large distortion in the strongly bonded complexes TA-TtR_3···NCM (Tt= Si and Ge). When these complexes are optimized at the fixed Tt···N distance of 3 Å, this distortion becomes smaller since the N-Tt-R angle is larger than 100° and the N-Tt bond has smaller elongation (Table S8).

5. Conclusions

When attached to a tetrazole ring, the SiR_3 group engages in much stronger tetrel bonds with an activated NCM base than does its C-analogues. The interaction energies of the former range upwards of 50 kcal/mol, while the latter are less than 8 kcal/mol. These strong tetrel bonds are fairly short, between 1.94 and 2.2 Å, as compared to 3 Å or more for CR_3. Formation of these Si···N TtBs induces a stretch of the internal N-Si bond by nearly 0.1 Å. These bonds are magnified when a BR_3 Lewis acid attaches itself to a N atom of the tetrazole ring. The C···N

TtBs enlarge to the 7-11 kcal/mol range, while the Si···N bonds climb above 60 kcal/mol. Some of these complexes can be thought of as containing a half-transferred SiR_3 group with nearly equivalent internal and external Si···N bond lengths.

Conflict of Interest

The authors declare no conflict of interest.

Acknowledgements

This work was supported by the Natural Science Foundation of Shandong Province (ZR2021MB123) and the US National Science Foundation (1954310).

References

1 M. S. Gargari, V. Stilinović, A. Bauzá, A. Frontera, P. McArdle, D. V. Derveer, S. W. Ng and G. Mahmoudi, *Chem. Eur. J*., 2015, ***21***, 17951–17958.

2 S. Mirdya, S. Roy, S. Chatterjee, A. Bauzá, A. Frontera and S. Chattopadhyay, *Cryst. Growth Des*., 2019, ***19***, 5869–5881.

3 A. Frontera and A. Bauzá, *Chem. Eur. J*., 2018, ***24***, 16582–16587.

4 X. García-LLinás, A. Bauzá, S. K. Seth and A. Frontera, *J. Phys. Chem. A,* 2017, ***121***, 5371–5376.

5 A. Bauzá, T. J. Mooibroek and A. Frontera, *ChemPhysChem,* 2015, ***16,*** 2496–2517.

6 A. Bauzá, J. Tiddo, T. J. Mooibroek and A. Frontera, *Angew. Chem. Int. Ed*., 2013, ***125***, 12543–12547.

7 A. Daolio, P. Scilabra, G. Terraneo and G. Resnati, *Coord. Chem. Rev*., 2020, ***413***, 213265.

8 V. R. Mundlapati, D. K. Sahoo, S. Bhaumik, S. Jena, A. Chandrakar and H. S. Biswal, *Angew. Chem. Int. Ed*., 2018, ***57***, 16496–16500.

9 S. Jena, J. Dutta, K. D. Tulsiyan, A, K, Sahu, S, S, Choudhury and H. S. Biswal, *Chem. Soc. Rev*., 2022, ***51***, 4261−4286.

10 J. Dutta, A. K. Sahu, A. S. Bhadauria and H. S. Biswal, *J. Chem. Inf. Model*., 2022, ***62***, 1998−2008.

11 S. S. Choudhury, S. Mahapatra and H. S. Biswal, *Green Chem*., 2022, ***24***, 4981−4990.

12 S. H. Jungbauer and S. M. Huber, *J. Am. Chem. Soc*., 2015, ***137***, 12110−12120.

13 Q. Z. Li, X. Guo, X. Yang, W. Z. Li, J. B. Cheng and H. B. Li, *Phys. Chem. Chem. Phys*., 2014, ***16***, 11617–11625.

14 M. X. Liu, Q. Z. Li, W. Z. Li and J. B. Cheng, *Struct. Chem*., 2017, ***28***, 823–831.

15 J. Mikosch, S. Trippel, C. Eichhorn, R. Otto, U. Lourderaj, J. X. Zhang, W. L. Hase, M. Weidemüller and R. Wester, *Science,* 2008, ***319***, 183–186.
16 S.J. Grabowski, *Phys. Chem. Chem. Phys*., 2014, ***16***, 1824–1834.
17 M.X. Liu, Q.Z. Li, J.B. Cheng, W.Z. Li and H.B. Li, *J. Chem. Phys*., 2016, ***145***, 224310.
18 A. Karim, N. Schulz, H. Andersson, B. Nekoueishahraki, A. C. C. Carlsson, D. Sarabi, A. Valkonen, K. Rissanen, J. Gräfenstein, S. Keller and M. Erdélyi, *J. Am. Chem. Soc*., 2018, ***140***, 17571−17579.
19 P. Sarkar, S. Das and S. K. Pati, *Inorg. Chem*., 2021, ***60***, 15180−15189.
20 S. P. Gnanasekar and E. Arunan, *J. Phys. Chem. A,* 2019, ***123***, 1168−1176.
21 K. J. Tielrooij, M. J. Cox and H. J. Bakker, *ChemPhysChem,* 2009, ***10***, 245–251.
22 O. Mó, M. Yáñez, I. Alkorta and J. Elguero, *J. Chem. Theory Comput*., 2012, ***8***, 2293−2300.
23 Y.Y. Wei, Q.Z. Li and S. Scheiner, *ChemPhysChem,* 2018, ***19***, 736–743.
24 M.C. Hou, Q.Z. Li and S. Scheiner, *Chem. Phys. Lett*., 2019, ***731***, 136584.
25 N. Liu, X.Y. Xie, Q.Z. Li and S. Scheiner, *ChemPhysChem,* 2021, ***22***, 2305–2312.
26 N. Liu, Q.Z. Wu, Q.Z. Li and S. Scheiner, *Phys. Chem. Chem. Phys*., 2022, ***24***, 1113–1119.
27 M. Yáñez, O. Mó, I. Alkorta and J. Elguero, *Chem. Eur. J*., 2013, ***19***, 11637–11643.
28 L. Albrecht, R. J. Boyd and O. Mo, *J. Phys Chem A,* 2014, ***118***, 4205–4213.
29 O. Mó, M. Yáñez and I. Alkorta, *Mol. Phys*., 2014, ***112***, 592–600.
30 X. Pang, C. Jiang, W. Xie and W. Domcke, *Phys. Chem. Chem. Phys.,* 2019, ***21***, 14073–14079.
31 S. Cybulski and S. Scheiner, *J. Am. Chem. Soc.,* 1987**,** ***109***, 4199–4206.
32 P. Chatterjee, A. K. Ghosh, M. Samanta and T. Chakraborty, *J. Phys. Chem. A,* 2018, ***122***, 5563–5573.
33 M. M. Szczesniak and S. Scheiner, *J. Chem. Phys.,* 1982**,** ***77***, 4586–4593.
34 A. Namslauer and P. Brzezinski, *FEBS Lett.,* 2004**,** ***567***, 103–110.
35 M. V. Vener and S. Scheiner, *J. Phys. Chem.,* 1995**,** ***99***, 642–649.
36 S. Scheiner, D. A. Kleier and W. N. Lipscomb, *Proc. Nat. Acad. Sci. USA,* 1975**,** ***72***, 2606–2610.
37 Y. Kim and K.H. Ahn, *Theor. Chem. Acc.,* 2001, ***106***, 171–177.
38 S. Scheiner, M. M. Szczesniak and L. D. Bigham, *Int. J. Quantum Chem.,* 1983, ***23***, 739–751.
39 C. Møller and M. S. Plesset, *Phys. Rev*., 1934, ***46***, 618−622.
40 S. F. Boys and F. Bernardi, *Mol. Phys*., 1970, ***19***, 553–566.
41 M. J. Frisch, G. W. Trucks, H. B. Schlegel, G. E. Scuseria, M. A. Robb, J. R. Cheeseman, G. Scalmani, V. Barone, B. Mennucci, G. A. Petersson, H. Nakatsuji, M. Caricato, X. Li, H. P. Hratchian, A. F. Izmaylov, J. Bloino, G. Zheng, J. L. Sonnenberg, M. Hada, M. Ehara, K.

Toyota, R. Fukuda, J. Hasegawa, M. Ishida, T. Nakajima, Y. Honda, O. Kitao, H. Nakai, T. Vreven, J. Montgomery, J. E. Peralta, F. Ogliaro, M. Bearpark, J. J. Heyd, E. Brothers, K. N. Kudin, V. N. Staroverov, R. Kobayashi, J. Normand, K. Raghavachari, A. Rendell, J. C. Burant, S. S. Iyengar, J. Tomasi, M. Cossi, N. Rega, J. M. Millam, M. Klene, J. E. Knox, J. B. Cross, V. Bakken, C. Adamo, J. Jaramillo, R. Gomperts, R. E. Stratmann, O. Yazyev, A. J. Austin, R. Cammi,C. Pomelli, J. W. Ochterski, R. L. Martin, K. Morokuma, V. G. Zakrzewski, G. A. Voth, P. Salvador, J. J. Dannenberg, S. Dapprich, A. D. Daniels, O. Farkas, J. B. Foresman, J. V. Ortiz, J. Cioslowski and D. J. Fox, Gaussian 09, RevisionD.01, Inc, Wallingford, CT **2009**.

42 F. A. Bulat, A. Toro-Labbé, T. Brinck, J. S. Murray and P. Politzer, *J. Mol. Model*., 2010, ***16***, 1679–1691.

43 T. Lu and F. W. Chen, *J. Comput. Chem*., 2012, ***33***, 580–592.

44 R. F. W. Bader, Atoms in Molecules: A Quantum Theory; Pearson Education Limited: London, *London*, 1990.

45 A. E. Reed, L. A. Curtiss and F. A. Weinhold, *Chem. Rev*., 1988, ***88***, 899–926.

46 M. W. Schmidt, K. K. Baldridge, J. A. Boatz, S. T. Elbert, M. S. Gordon, J. H. Jensen, S. Koseki, N. Matsunaga, K. A. Nguyen, S. J. Su, T. L. Windus, M. Dupuis and J. A. Montgomery, *J. Comput. Chem*., 1993, ***14***, 1347–1363.

47 P. F. Su and H. Li, *J. Chem. Phys*., 2009, ***131***, 014102.

48 S. J. Grabowski, *ChemPhysChem,* 2015, ***16***, 1470–1479.

49 D. Mani and E. Arunan, *Phys. Chem. Chem. Phy*s., 2013, ***15***, 14377–14383.

50 R. C. Trievel and S. Scheiner, *Molecules,* 2018, ***23***, 2965–2981.

51 V.L. Heywood, T.P.J. Alford, J.J. Roeleveld, S. J. L. Deprez, A. Verhoofstad, J. I. van der Vlugt, S. R. Domingos, M. Schnell, A. P. Davis and T. J. Mooibroek, *Chem. Sci.,* 2020, ***11***, 5289–5293.

52 Y.X. Wei, H.B. Li, J.B. Cheng, W.Z. Li and Q.Z. Li, *Int. J. Quantum Chem.,* 2017, ***117***, e25448.

53 A. Bauzá, T. J. Mooibroek and A. Frontera, *Chem. Rec*., 2016, ***16***, 473–487.

54 S. Scheiner, *J. Phys. Chem. A,* 2017, ***121***, 5561–5568.

55 M. Marín-Luna, I. Alkorta and J. Elguero, *Theor. Chem. Acc*., 2017, ***136***, 41–48.

56 M. Marín-Luna, I. Alkorta and J. Elguero, *J. Phys. Chem. A,* 2016, ***120***, 648–656.

57 W. Zierkiewicz, M. Michalczyk and S. Scheiner, *Phys. Chem. Chem. Phys*., 2018, ***20***, 8832–8841.

58 A. Bauzá, T. J. Mooibroek and A. Frontera, *Angew. Chem. Int. Ed*., 2013, ***52***, 12317–12321.

59 W. Zierkiewicz, M. Michalczyk, R. Wysokiński and S. Scheiner, *Molecules,* 2019, ***24***, 376.

60 W. Zierkiewicz, A. Grabarz, M. Michalczyk and S. Scheiner, *ChemPhysChem,* 2021, ***22***, 924–934.

61 M. Liu, Q. Li and S. Scheiner, *Phys. Chem. Chem. Phys*., 2017, ***19***, 5550–5559.

62 R. Wysokiński, M. Michalczyk, W. Zierkiewicz and S. Scheiner, *Phys. Chem. Chem. Phys*., 2019, ***21***, 10336–10346.

63 D. J. Duchamp and C. G. Chidester, *Acta Cryst. B,* 1972, ***28***, 173–180.

64 A. P. M. Robertson, S. S. Chitnis, S. Chhina, S., H. J. Cortes C, B. O. Patrick, H. A. Jenkins and N. Burford, *Can. J. Chem.,* 2016, ***94***, 424–429.

65 S. Bhattarai, D. Sutradhar and A. K. Chandra, *ChemPhysChem,* 2022, ***23***, e202200146.

66 W. Zierkiewicz, M. Michalczyk and S. Scheiner, *Molecules,* 2018, ***23***, 1416.

67 J. Zhang, Q. Hu, Q. Li, S. Scheiner and S. Liu, *Int. J. Quantum Chem*., 2019, ***119***, e25910.

68 S.J. Grabowski and J. Leszczynski, *Chem. Phys*., 2009, ***355***, 169-176.

69 T. Kar and S. Scheiner, *J. Phys. Chem. A,* 2004, ***108***, 9161–9168.

70 S. S. Xantheas, *Chem. Phys*., 2000, ***258***, 225–231.

71 M. X. Liu, L. Yang, Q. Z. Li, W. Z. Li, J. B. Cheng, B. Xiao and X. F. Yu, *J. Mol. Model*., 2016, ***22***, 192.

72 M. C. Hou, Y. F. Zhu, Q. Z. Li and S. Scheiner, *ChemPhysChem,* 2020, ***21***, 212–219.

73 D.L. Fiacco and K.R. Leopold, *J. Phys. Chem. A,* 2003, ***107***, 2808–2814.